

A macrophage uptaking near-infrared chemical probe CDnir7 for *in vivo* imaging of inflammation†

Cite this: *Chem. Commun.*, 2014, 50, 6589

Received 19th March 2014,
Accepted 2nd May 2014

DOI: 10.1039/c4cc02038c

www.rsc.org/chemcomm

Nam-Young Kang,‡^a Sung-Jin Park,‡^a Xiao Wei Emmiline Ang,^a Animesh Samanta,^a Wouter H. P. Driessen,^b Vasilis Ntziachristos,^c Kristine O. Vasquez,^d Jeffrey D. Peterson,^d Seong-Wook Yun*^a and Young-Tae Chang*^{ae}

Visualization of macrophages in live animals has been of great interest for a better understanding of inflammation. We developed a near infrared (NIR) probe CDnir7 that can selectively detect macrophages and visualize inflammation *in vivo* using the IVIS spectrum, Fluorescence Molecular Tomography (FMT) and Multi-Spectral Optoacoustic Tomography (MSOT).

Inflammation is an immune response in the body normally triggered by infection, tissue damage or allergic substances. For the development of inflammation in tissues, migration of immune cells, including monocytes from the blood, to the tissue is essential. Infiltrating monocytes then differentiate into macrophages and function primarily as scavengers of foreign pathogenic organisms, apoptotic cells and dead cell debris and secrete pro- or anti-inflammatory cytokines.¹ Macrophages are often recruited by solid tumors to become tumor-associated macrophages which promote tumor progression and metastasis by secreting growth factors for tumor cell proliferation and angiogenesis.² Therefore, monitoring the behavior of macrophages in inflammation and tumor is crucial for the diagnosis and prognosis of a wide range of diseases.

Methodologically, macrophage imaging is conducted by administration of macrophages that are pre-labelled *in vitro*, or by directly injectable probes that selectively label macrophages in inflamed areas.³ Although employing *in vitro* labeled macrophages is the most common method in current medical practice, the procedure for isolating, labeling and reinjecting macrophages is complicated,

often resulting in high variation in data quality and contamination problems. Moreover, leakage of labeling agents from the injected cells can generate false background signals by labeling surrounding cells non-specifically. On the other hand, cell type specific probes can be directly administered into the body without the need for extra cell preparation steps. Currently, only a few injectable imaging probes based on fluorescently labelled magnetic nanoparticles for phagocytic uptake⁴ or extracellular protease substrate peptides⁵ have been developed to visualize macrophages in the body by optical imaging.

The conventional approach for fluorescent probe development, however, has been limited to optical reporters conjugated to target-specific molecules such as antibodies, oligonucleotides and peptides. As an alternative approach, we have developed a diversity oriented fluorescence library approach (DOFLA) using structurally diverse and intrinsically fluorescent small organic dyes. By screening the DOFL in many different types of living cells, we have discovered fluorescent dyes that selectively stain only certain types of cells such as embryonic stem cells, neural stem cells, basophils, pancreatic alpha cells and beta cells.⁶ While successful both in *in vivo* and *in vitro* imaging using DOFLA, a drawback of these previously reported dyes is the fact that their maximum excitation and emission wavelengths have generally been between 400 and 600 nm and thus they have had limited tissue penetration capability, making them less suitable for *in vivo* live animal imaging. To overcome this physico-optical limitation, we recently developed photostable NIR compound libraries⁷ and applied these for macrophage selective probe development. Herein we report the first NIR macrophage uptaking probe CDnir7 and its application of *in vivo* animal imaging in various modality and disease models.

For the primary screening of NIR compounds that selectively stains macrophages *versus* leukocytes, we plated RAW 264.7 (mouse macrophage cell line) and as the negative control, primary mouse splenocytes (a mixture of various types of leukocytes) side by side in 96-well plates. The cells were incubated with two hundred NIR compounds⁷ at 1 μ M for 1 hour and the epi-fluorescence microscopic image of each well was acquired. The fluorescence intensity of the cells was analyzed using image analysis software as well as by manual observation. Although a small number of macrophages were expected to be in the splenocyte culture (approximately 10%), their

^a Singapore Bioimaging Consortium, Agency for Science, Technology and Research, 11 Biopolis Way, # 02-02 Helios, Singapore 138667, Singapore.

E-mail: yun_seong_wook@sbc.a-star.edu.sg

^b iThera Medical, GmbH, Munich, Germany

^c Institute for Biological and Medical Imaging (IBMI), Helmholtz Centre Munich Chair of Biological Imaging (CBI), Technische Universität Munich, Germany

^d Life Sciences & Technology, PerkinElmer, Inc, Boston, Massachusetts, USA

^e Department of Chemistry & Med Chem Program, Life Sciences Institute, National University of Singapore, 3 Science Drive 3, Singapore 117543, Singapore.

E-mail: chmcyt@nus.edu.sg; Web: http://ytchang.science.nus.edu.sg

† Electronic supplementary information (ESI) available: Experimental procedures, spectroscopic data, cell image data. See DOI: 10.1039/c4cc02038c

‡ These authors contributed equally.

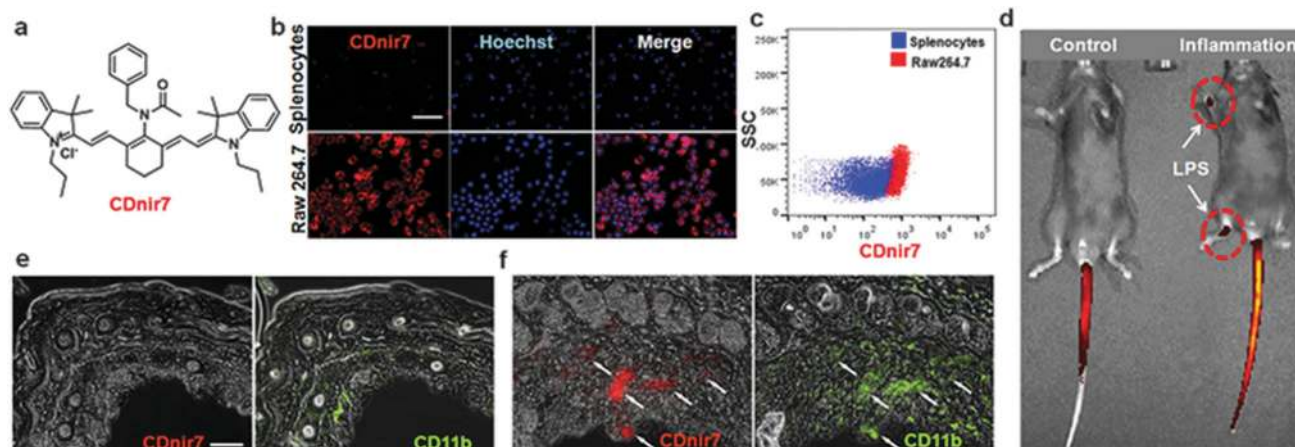


Fig. 1 Discovery of the NIR fluorescence probe **CDnir7** and *in vivo* imaging of inflammation. (a) Chemical structure of **CDnir7**. (b) Fluorescence images of mouse splenocytes and the macrophage cell line Raw 264.7. (c) Flow cytometry dot plot images of splenocytes and Raw 264.7. (d) **CDnir7** detection in inflamed regions of live mouse paws using the IVIS spectrum. LPS (1 mg mL⁻¹, 200 μL) was injected into the right paws 2 days prior to the imaging. **CDnir7** (100 μM, 250 μL, 1% PEG and 0.1% Tween 20 in PBS) was injected *via* the tail vein and the image was obtained 30 minutes later. (e) Immunostaining images of **CDnir7** and CD11b using the left rear foot (control region, e) and the right rear foot (f). Scale bar: 50 μm.

contribution to the total fluorescence signal was negligible in the screening. From the cell based screening, we identified 5 hit compounds that stained RAW 264.7 cells more strongly than primary splenocytes in epi-fluorescence microscopy imaging (Fig. 1b and Fig. S1, ESI[†]). The five hit compounds were then evaluated for their efficiency in detecting inflammation *in vivo* using a well established mouse model. We induced acute inflammation in mice by injecting lipopolysaccharide (LPS) into the paws (2 days) and then administered the hit compounds by tail vein injection. The fluorescence signals were monitored by the IVIS spectrum imaging system using appropriate NIR filters, and we identified one compound **CyNA-E10**, as the best imaging probe *in vivo* (Fig. 1d) based on its strong fluorescence signal only at the LPS injected site. Interestingly, the other four hit compounds did not show a clear localization in the inflammation site, when injected into this mouse model. The selected *in vivo* probe compound, **CyNA-E10** was dubbed **CDnir7** (Compound of Designation near infrared 7; Fig. 1a) and its optical properties were fully characterized ($\lambda_{\text{ex}}/\lambda_{\text{em}} = 806/821$ nm in DMSO; extinction coefficient = 198 500 M⁻¹ cm⁻¹; quantum yield = 0.14 in Scheme S1 & Fig. S6, ESI[†]). In addition to fluorescence imaging, **CDnir7** demonstrated a clear separation of macrophages from splenocytes using flow cytometry analysis (Fig. 1c). Using the *in vivo* mice model, we further confirmed that **CDnir7** specifically stained macrophage cells in the inflamed paw by immunostaining histological sections for the macrophage marker CD11b. Strong **CDnir7** signals were observed only in the inflamed paw and colocalized with CD11b positive cells (Fig. 1f), whereas the control area remains largely negative for CD11b and **CDnir7** (Fig. 1e). **CDnir7** did not show any apparent toxicity at the working concentration (1 μM) over 24 hours in macrophage cells (Fig. S2, ESI[†]) and in the liver, kidney and spleen tissue from **CDnir7** injected mice even at 10 times the working concentration (Fig. S3–S5, ESI[†]). There are many unpredictable factors that hinder the successful application of imaging probes identified by cell-based screening to whole animal *in vivo* imaging. In cell culture, only a few cell types are compared as negative control, under defined conditions and unbound probes can be simply removed by exchanging the

culture media. In a living mammalian organism, however, the probes should selectively stain the target cells among high numbers of different types of cells, and unbound probes need to be either metabolized or excreted from the body. These differences between cell culture and whole organism likely explain why the other four primary hit compounds did not show specific signals in the inflamed regions of the mice.

For further quantitative analysis of **CDnir7** staining for inflammation imaging in mice, we monitored the signal of **CDnir7** by a tomographic fluorescence imaging method, FMT. For an acute animal model, we induced inflammation in mice by injecting carrageenan (CG) into a footpad, an approach that

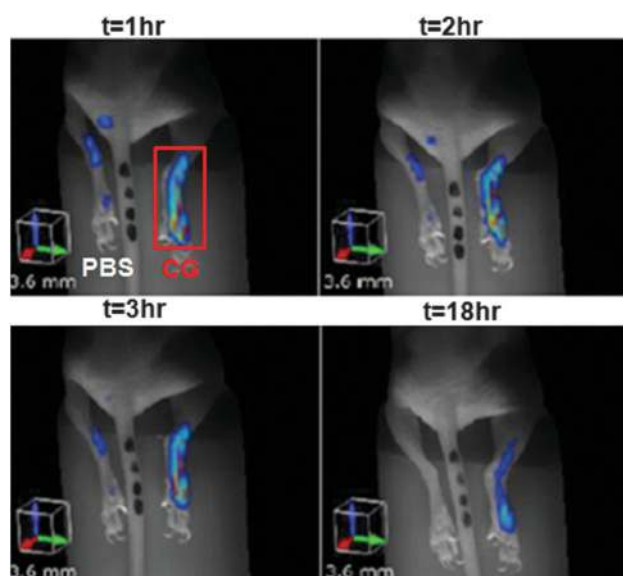


Fig. 2 Fluorescence Molecular Tomographic (FMT) imaging of paw inflammation by **CDnir7**. Time-lapse FMT imaging of **CDnir7** in edema induced by the injection of 1% carrageenan (CG-marked with red box) into the right hind footpad. The left paw was injected with PBS as the internal control. Mice ($n = 2$) were imaged by FMT at 1, 2, 3 and 18 h after **CDnir7** injection.

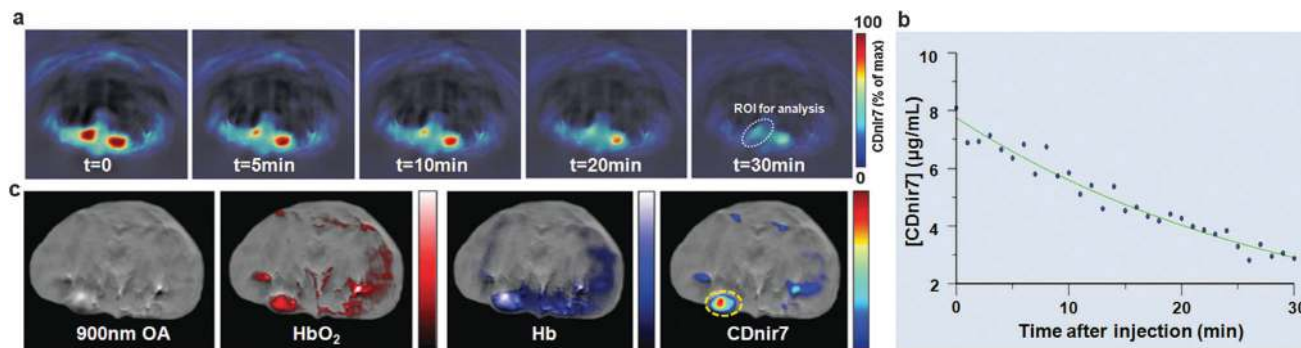


Fig. 3 *In vivo* imaging of **CDnir7** kinetics and accumulation in breast tumor by Multi-Spectral Optoacoustic Tomography (MSOT). (a) Time lapse MSOT imaging of **CDnir7** signal in jugular veins (ROI for half-life determination marked with white circles). (b) MSOT image-based quantification of **CDnir7** in jugular veins over time. (c) Single wavelength optoacoustic (OA) image at 900 nm before **CDnir7** injection (far left) and spectrally unmixed signals: hemoglobin (oxygenated, HbO₂; deoxygenated, Hb) and **CDnir7** in the orthotopic breast tumor.

yields neutrophil and macrophage influx into the injected region. After administration of **CDnir7** into the blood stream through tail vein injection, we measured the thickness of the paws and acquired fluorescence images periodically up to 18 hours. CG injection caused a rapid noticeable swelling in the paws, while PBS, injected as a control, caused only slight swelling. A significantly stronger fluorescence signal was detectable in the CG-injected paw compared to the PBS control at 1 hour after **CDnir7** administration. The fluorescence signal in regions of CG-induced edema remained stable between 1 and 3 h and then declined by 66% after 18 h. Despite the decline in fluorescence intensity, the signal difference between inflamed and control paws was clearly detectable (Fig. 2), supporting the utility of this probe in detecting and quantifying inflammation. Between paw thickness and **CDnir7** signal intensity, there was an excellent linear correlation (Fig. S7, ESI[†]). For broader application of the NIR probe, we also assessed the capability of **CDnir7** for *in vivo* photoacoustic imaging by MSOT. First we tested whether the absorbance spectrum and molar extinction coefficient of **CDnir7** were affected by serum albumin, which has been known to bind to a wide range of organic compounds in the blood potentially affecting their function and property. In the presence of 10% bovine serum albumin (BSA) in PBS, **CDnir7** displayed maximum absorbance at 800 nm which was slightly (15 nm) red-shifted compared to the value in PBS (Fig. S8a and b, ESI[†]). In scattering agar phantoms (1.2% agar, 1% intralipid), **CDnir7** showed a strong photoacoustic signal and excellent linearity at concentrations ranging from 0.15 μM to 5 μM regardless of the presence of BSA (Fig. S8c and d, ESI[†]).

To study the pharmacokinetics of **CDnir7** by deep tissue *in vivo* imaging, we intravenously infused **CDnir7** into naïve mice and continuously monitored the neck region of the mice. The plasma half-life of **CDnir7**, determined by spectral unmixing using the linear regression of the signal from a jugular vein, was 21 min (Fig. 3a and b). Plasma half-life of **CDnir7** measured using MSOT is much shorter than those of nanoparticle-based macrophage imaging probes, e.g., ~ 3.9 h for 89 Zr-labeled dextran nanoparticles,⁸ and ~ 10 h for cross-linked iron oxide.⁹ This short plasma half-life of **CDnir7** makes the retained probe in macrophages rapidly distinguishable after injection of the probe, thus offering an advantage over nanoparticles used to detect phagocytic cells. We next studied the accumulation of **CDnir7**

in mice bearing orthotopic 4T1 breast tumors, which are known to recruit large numbers of tumor-associated macrophages. In the tumor region, which was identified by signals from oxygenated and deoxygenated hemoglobin, the apparent accumulation of **CDnir7** was observed (Fig. 3c). When the tumor region was monitored kinetically, **CDnir7** accumulation reached a maximum within 10 min and was detectable beyond 3 hours (Fig. S9, ESI[†]). In comparison to tumor imaging kinetics, the kinetic changes in the **CDnir7** signal in a nearby blood vessel were significantly different, decreasing rapidly in the first 5 minutes and more slowly thereafter.

In conclusion, we developed the first macrophage-targeted NIR probe and demonstrated *in vivo* imaging in mice using various modalities, IVIS, FMT and MSOT. Using *in vivo* imaging in various modalities, **CDnir7** provides a powerful fluorescence imaging probe for the detection and quantification of inflammation occurring *in situ* in regions of disease.

This study was supported by an intramural funding from A*STAR (Agency for Science, Technology and Research, Singapore) Biomedical Research Council and a Singapore Ministry of Education Academic Research Fund Tier 2 (MOE2010-T2-2-030).

Notes and references

- K. J. Moore, F. J. Sheedy and E. A. Fisher, *Nat. Rev. Immunol.*, 2013, **13**, 709–721.
- P. Allavena and A. Mantovani, *Clin. Exp. Immunol.*, 2012, **167**, 195–205.
- F. J. Van Hemert, C. Voermans, B. L. Van Eck-Smit and R. J. Bennink, *Q. J. Nucl. Med. Mol. Imaging*, 2009, **53**, 78–88.
- R. Weissleder, K. Kelly, E. Y. Sun, T. Shtatland and L. Josephson, *Nat. Biotechnol.*, 2005, **23**, 1418–1423.
- R. Weissleder, C. H. Tung, U. Mahmood and A. Bogdanov Jr., *Nat. Biotechnol.*, 1999, **17**, 375–378.
- N. Y. Kang, H. H. Ha, S. W. Yun, Y. H. Yu and Y. T. Chang, *Chem. Soc. Rev.*, 2011, **40**, 3613–3626.
- A. Samanta, M. Vendrell, R. Das and Y. T. Chang, *Chem. Commun.*, 2010, **46**, 7406–7408; A. Samanta, K. K. Maiti, K. S. Soh, X. Liao, M. Vendrell, U. S. Dinis, S. W. Yun, R. Bhuvaneshwari, H. Kim, S. Rautela, J. Chung, M. Olivo and Y. T. Chang, *Angew. Chem., Int. Ed.*, 2011, **50**, 6089–6092; S. C. Lee, D. Zhai, P. Mukherjee and Y. T. Chang, *Materials*, 2013, **6**, 1779–1788.
- E. J. Keliher, J. Yoo, M. Nahrendorf, J. S. Lewis, B. Marinelli, A. Newton, M. J. Pittet and R. Weissleder, *Bioconjugate Chem.*, 2011, **22**, 2383–2389.
- P. Wunderbaldinger, L. Josephson and R. Weissleder, *Bioconjugate Chem.*, 2002, **13**, 264–268.